In Proceedings of the ISMA 2006 International Conference on Noise and Vibration Engineering, Leuven, Belgium, September 2006

In-flight modal analysis – a comparison between sweep and turbulence excitation

Bart Peeters[1], Tim De Troyer[2], Patrick Guillaume[3], Herman Van der Auweraer[1]
[1]LMS International
Interleuvenlaan 68, B-3001 Leuven, Belgium
e-mail: **bart.peeters@lms.be**

[2]Erasmushogeschool, Department IWT
Nijverheidskaai 170, B-1070 Brussel, Belgium

[3]Vrije Universiteit Brussel, Department of Mechanical Engineering
Pleinlaan 2, B-1050 Brussel, Belgium

Abstract

At the end of the development cycle, a new aircraft is certified by means of in-flight flutter tests. These tests consist of flying the aircraft at different airspeeds and measuring the accelerations at a limited number of locations on the aircraft structure. The scope is to open the flight domain by verifying that the aircraft does not suffer from aero-elastic instabilities such as flutter.

In this paper, some modern frequency-domain modal parameter estimation methods are applied to in-flight data of a large aircraft. Traditional sine sweep excitation was applied at the control surfaces. However, during the test the aircraft passed through a turbulent zone. The sweep excitation was immediately stopped, but the on-board data acquisition system continued to record the aircraft vibration response. After quitting the turbulent zone, the sweep test was reinitiated. The present data thus allows for a comparison between artificial and natural excitation. More specifically, aspects such as data pre-processing, easiness of the parameter extraction process and the accuracy of the results are investigated.

1 Introduction

The development cycle of a new aircraft consists of several modelling and testing stages: structural finite element (FE) modelling, ground vibration testing (GVT), computational fluid dynamics (CFD) modelling, wind tunnel testing, and in-flight tests. These flight (vibration) tests allow the validation of the analytical models under various real flight conditions and, more important, allow to assess the aero-elastic interaction, as a function of airspeed and altitude, between the structure and the aerodynamic forces as they may lead to a sudden unstable behaviour known as flutter. Flutter shows up in the vibration signals as apparent negative damping and corresponding sudden increase of the vibration amplitudes. For economic and safety reasons (i.e. to avoid a loss of the aircraft), it is evidently avoided that an aircraft goes into flutter during an in-flight test, but it has to be certified that it has sufficient flutter margin when flying at the different points of the flight envelope where it is designed for. To determine this margin, typically, the trends of eigenfrequencies and damping ratios of the critical modes as a function of airspeed are carefully studied. This explains the need to perform a modal analysis during the flight. More background information on flight flutter testing can be found in [1][2].

When exciting the aircraft artificially during the flight, a reference signal representative for the force input is typically recorded, Frequency Response Functions (FRFs) can be estimated and classical modal analysis can be applied. Exciting the aircraft during flight is possible e.g. by installing rotating vanes at the wing tips or by adding a broadband signal to the control surface signal. Recently, there was an increased interest in using natural turbulences as excitation. It is practically impossible to measure this ambient excitation and, by consequence, the outputs (i.e. aircraft responses) are the only information that can be passed to the system identification algorithms. In this case one speaks of *Operational Modal Analysis*.

The paper is organized as follows. In Section 2, a short overview of poly-reference frequency-domain modal parameter estimation methods is given. Section 3 introduces the in-flight aircraft vibration data that will be used to illustrate the concepts of this paper. The data combines natural turbulence and artificial sine sweep excitation at the same flight conditions. Section 4 is the main part of the paper and discusses the application of classical modal analysis, the influence of sweep data pre-processing on the estimation results, and the application of Operational Modal Analysis. Also the classical and Operational Modal Analysis results will be compared.

2 Frequency-domain modal parameter estimation

The "poly-reference" frequency-domain system identification methods [3] considered in this paper identify following so-called right matrix-fraction model:

$$[H(\omega)] = \sum_{r=0}^{p} z^r [\beta_r] . \left(\sum_{r=0}^{p} z^r [\alpha_r] \right)^{-1} \tag{1}$$

where $H(\omega) \in \mathbb{C}^{l \times m}$ is the Frequency Response Function (FRF) matrix that is estimated in a non-parametric way from the measured vibration data (see also Section 4.1.2); $[\beta_r] \in \mathbb{R}^{l \times m}$ are the numerator matrix polynomial coefficients; $[\alpha_r] \in \mathbb{R}^{m \times m}$ are the denominator matrix polynomial coefficients; l is the number of outputs; m is the number of inputs; p is the model order. Note that a so-called z-domain model (i.e. a frequency-domain model that is derived from a discrete-time model) is used in (1), with $z = \exp(j\omega\Delta t)$ and Δt being the sampling time.

In modal parameter estimation applications of frequency-domain system identification, the right matrix fraction model (1) is, after identification, converted to a modal model:

$$[H(\omega)] = \sum_{i=1}^{n} \frac{\{v_i\} < l_i^T >}{j\omega - \lambda_i} + \frac{\{v_i^*\} < l_i^H >}{j\omega - \lambda_i^*} \tag{2}$$

where n is the number of modes (it relates to the right matrix-fraction model order p as $2n = pm$); $\bullet^*$ is the complex conjugate of a matrix; $\{v_i\} \in \mathbb{C}^l$ are the mode shapes; $< l_i^T > \in \mathbb{C}^m$ are the so-called *participation factors* and λ_i are the poles, which are occurring in complex-conjugated pairs and are related to the eigenfrequencies ω_i and damping ratios ξ_i as follows:

$$\lambda_i, \lambda_i^* = -\xi_i \omega_i \pm j\sqrt{1-\xi_i^2}\,\omega_i \tag{3}$$

Different procedures exist to identify a right matrix fraction model from measured FRFs. Equation (1) can be written down for all values ω of the frequency axis of the FRFs. Basically, the unknown model coefficients $[\alpha_r], [\beta_r]$ can be found as the Least-Squares (LS) solution of these equations after linearization. The PolyMAX algorithm is such a LS implementation which has been memory and time optimized and uses a particular parameter constraint. More details about the PolyMAX method can be found in [4][5]. Mainly due its user-friendliness (the method yields extremely clear stabilization diagrams), PolyMAX is considered as an important breakthrough in modal parameter estimation.

Instead of solving a LS problem with a particular parameter constraint, it is also possible to constrain the Frobenius norm of the coefficients to the identity matrix. This leads to the poly-reference Total Least Squares (TLS) approach.

Theoretically, deterministic methods are less suited for highly noisy data such as flutter test measurements. Therefore, stochastic poly-reference frequency-domain estimators were recently derived [6]. If noise information is available, an important improvement in efficiency can be obtained [7] by using the covariance matrix of the measured FRFs.

The Generalized Total Least Squares (GTLS) estimator right multiplies the TLS cost function with the square root of the covariance matrix and then calculates a generalized eigenvalue decomposition.

A further improvement can be obtained by weighing iteratively with an estimate of the "optimal" Maximum Likelihood (ML) weighting. The weighting term involves, next to noise information, the denominator coefficients $[\alpha_r]$ estimated in the previous iteration step. The enhanced parameter estimates are then used to calculate a new weighting, resulting in new estimates, and so on. This weighting applied to a (T)LS estimator is called the Iterative Quadratic Maximum Likelihood (IQML) estimator, if applied to a GTLS estimator it is referred to as the Bootstrapped Total Least Squares (BTLS) estimator [8]. As shown in [7], two iterations (i.e. one initial estimate and one update with the weighting calculated using the denominator coefficients derived in the initial estimate) generally suffice to realize a significant improvement. It is important to note that the IQML-estimator can be formulated in a Least-Squares and Total-Least-Squares sense.

More details about the methods can be found in [6][7][9]. All these deterministic and stochastic estimators will be applied to in-flight aircraft data in Section 4.1 and Section 4.2.

3 In-flight vibration data: an interesting experiment

In this paper, some real in-flight vibration data is used to verify the effectiveness of the proposed algorithms. A large aircraft was excited by injecting a sine sweep signal in the outer aileron control signals. However, during the test the aircraft passed through a turbulent zone. The sweep excitation was immediately stopped, but the on-board data acquisition system continued to record the aircraft vibration response. After quitting the turbulent zone, the sweep test was reinitiated. The present data thus allows for a comparison between artificial and natural excitation. As inputs, either the sine sweep generator signal or the angles at the control surfaces can be taken, the outputs are acceleration response measurements at various locations at the airplane: fuselage, engines, wings, tail plane, fin … Upon indication by the aircraft manufacturer, data from 19 accelerometers were analysed. Some time histories are represented in Figure 1. For confidentiality reasons, no absolute quantities are given in this paper. The aircraft response due to turbulences has the same order of magnitude as the responses due to control surface excitation. At the tail, the turbulence response is even larger as, during the control surface excitation test, the wing input does not seem to excite the tail very well. This is confirmed when looking at the FRFs and coherences in Figure 2. These are computed by using only data from the 2nd sweep (after passing the turbulent zone). The generator signal was considered as reference signal. At tail plane and especially the fin, the coherence is very low at a large part of the frequency band of interest.

Also represented in Figure 2 are the transfer functions between the generator signal and the control surface angles. The amplitude is very flat in the frequency range of interest, providing the motivation to use the generator signal as reference. Both transfer functions have opposite phase, indicating that an anti-symmetric sweep was applied (i.e. excitation at both wings in opposite phase). Note that, in principle, only the anti-symmetric wing bending modes will be present in the estimated FRFs. It is easy to show that these FRFs referencing to a single generator signal which was sent in opposite phase to both wing control surfaces equals:

$$H = H_{wing\ 1} - H_{wing\ 2} \tag{4}$$

where $H_{wing\ X}$ represents the FRFs referencing to wing "*X*" excitation.

Figure 3 compares the spectra estimated during the turbulent zone with the FRFs at the 2nd sweep. Roughly the same dynamics (e.g. location of resonances) are observed when comparing power and cross spectra with the FRFs. This provides an intuitive justification for the application of Operational Modal Analysis (Section 4.2).

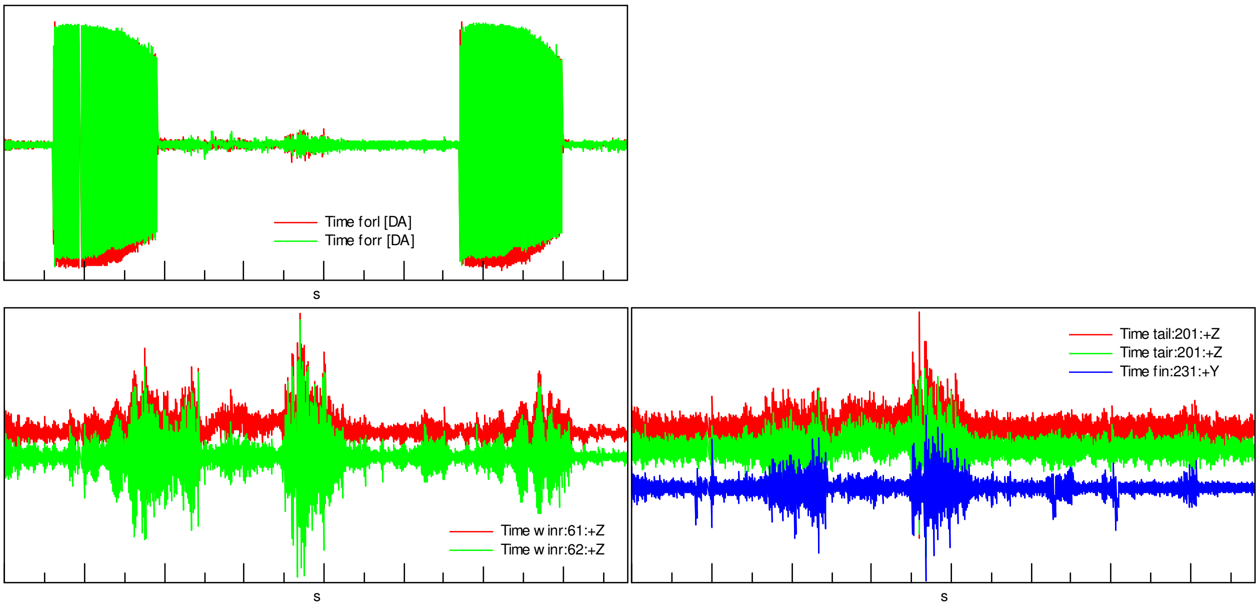

Figure 1: In-flight vibration data. (Top) input reference signals (angles at control surface); (Bottom) typical responses due to control surface and turbulence excitation; (Bottom-Left) wing tip response; (Bottom-Right) tail plane and fin response.

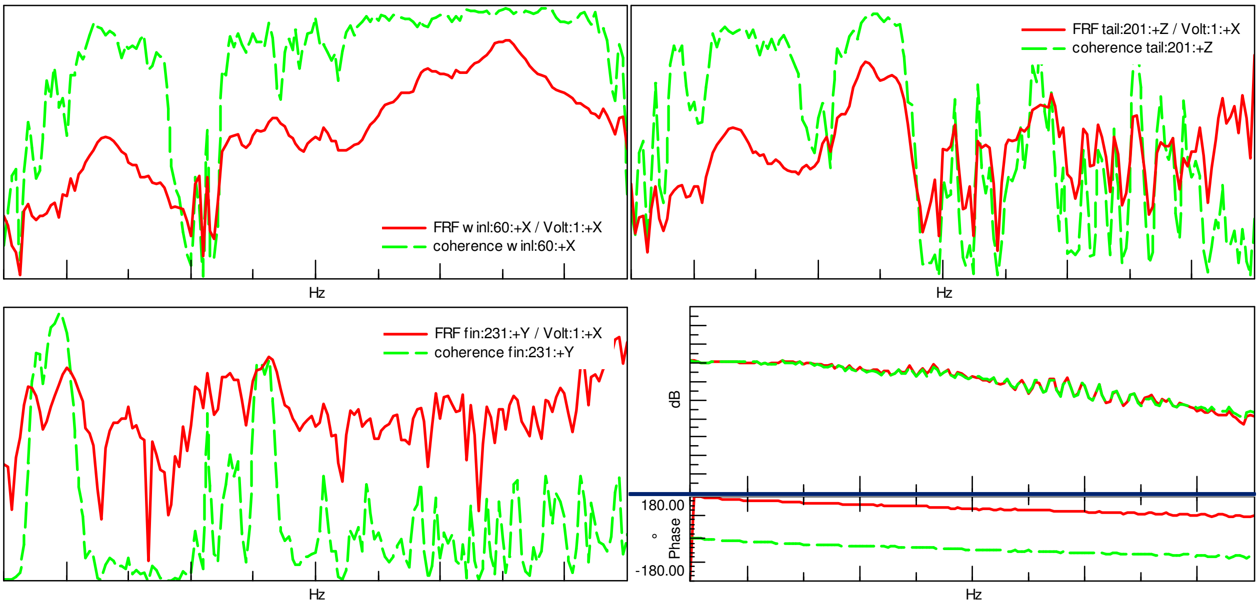

Figure 2: FRFs (full – red) and coherences (dashed – green): wing tip – tail plane – fin. The 4th picture represents the two transfer functions between sweep generator signals and actually measured control surface angles.

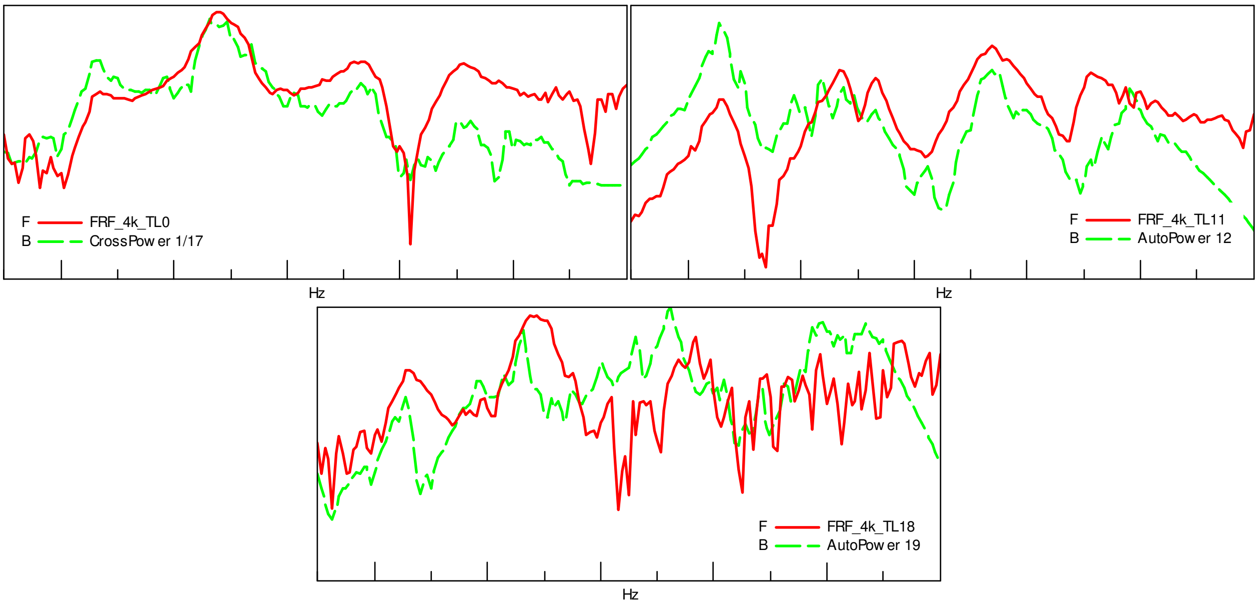

Figure 3: FRF (full – red) versus spectra (dashed – green): fuselage – wing tip – tail plane response.

4 Modal parameter estimation

In this section, the in-flight airplane modal parameters are estimated from the data introduced in Section 3. Section 4.1 applies FRF-based modal parameter estimation to the sweep excitation part of the data; Section 4.2 applies cross-spectra based modal parameter estimation to the turbulence part of the data; and, finally, both results are compared in Section 4.3.

4.1 Classical modal analysis applied to sweep FRF data

4.1.1 PolyMAX

As starting point for assessing the stochastic frequency-domain estimators, the PolyMAX method is applied to 19 aircraft FRFs. The non-parametric FRFs are computed as the well-known H1-estimate based on cross and power spectra obtained using Welch's averaged periodogram method with block size $N/2$ (see also Section 4.1.2 for a comparison with other block sizes), an overlap of 80% and applying a Hanning window.

The PolyMAX stabilization diagram is shown in Figure 4, clearly revealing the main feature of PolyMAX: the diagram is extremely clear, making it very easy to select the physical poles. Evidently, this is very relevant for the time-critical process of parameter estimation during flight. The six clearest modes that can be found in Figure 4 are considered as reference modes throughout this paper. Figure 5 confronts the measured FRFs with the FRFs synthesized from the estimated modal parameters; i.e. left hand side of (2) versus right-hand side of (2). The good correspondence indicates that the major dynamic characteristics have been extracted from the data.

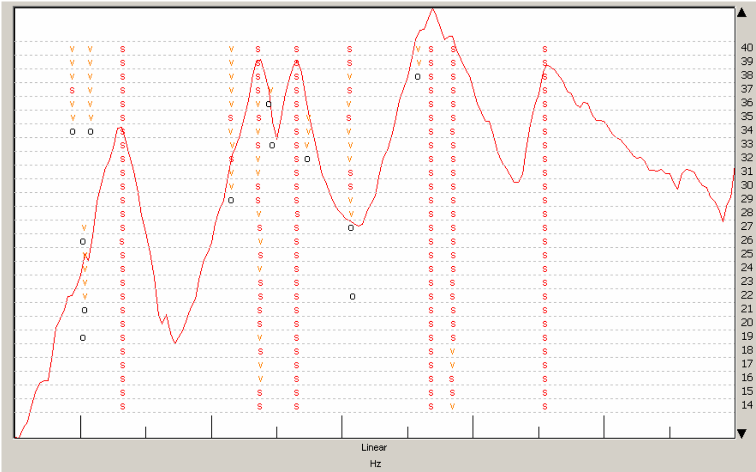

Figure 4: Stabilization diagram obtained by applying PolyMAX to in-flight aircraft data pre-processed to FRFs.

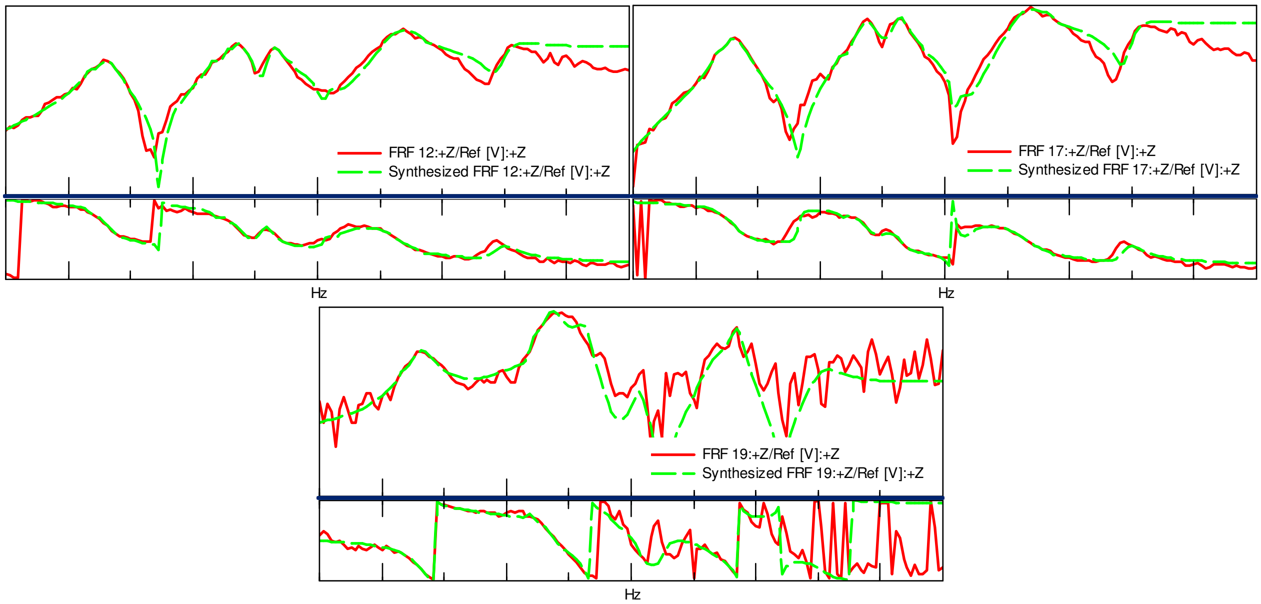

Figure 5: Measured (full – red) versus synthesized FRFs (dashed – green): right wing tip – left wing tip – tail plane.

4.1.2 Influence of pre-processing

As in in-flight modal analysis, the accuracy of the estimated eigenfrequencies and mainly the damping ratios is of utmost importance, it is worth investigating the influence of the data pre-processing on the estimated modal parameters.

While keeping the other pre-processing parameters (overlap, window type) constant, the block size is varied. Four different block sizes are used to estimate the FRFs: *N*, *N*/2, *N*/4, *N*/8. Again, PolyMAX was applied to the 4 datasets. The results are represented in Figure 6. Whereas the frequency variations remain small (±2%), the damping ratios dramatically (+200%) increase with decreasing block size. This is due to the relatively larger impact of the Hanning window. It is well-known that such a window leads to biased damping estimates (damping ratios too high), but it remains interesting to observe the impact in this particular case.

At first sight, a solution could be to take the block size as large as possible. However, a disadvantage of a large block size (e.g. *N*) is that not many averages can be computed and, hence, the FRFs are more affected by noise, which will make the mode extraction more difficult and again lead to biased estimates. As stated before, a disadvantage of a small blocksize is that the data will be more affected by the Hanning window and, hence, the estimated damping ratios will be biased. In [9], a workaround for this trade-off between noise and leakage effects is proposed. The idea is to first estimate the FRFs using a large block size, so suffering less from leakage and Hanning window bias, but suffering more from noise. The noise is reduced in a 2nd step by converting the FRFs to Impulse Response Functions (IRFs). The noise, appearing mainly in the higher time samples of the IRFs, is then reduced by applying a rectangular window. So the higher time samples are simply ignored. A new FRF can than be obtained by applying a DFT to the first IRF samples. This new FRF has a less fine frequency resolution, but noise effects are suppressed. In [9], it is furthermore demonstrated that the use of a rectangular window leads to biased participation factors, while the other modal parameters remain unchanged. However, a closed-form expression exists for this bias so that it can be easily removed.

The benefit of this approach is illustrated in Figure 7. The small block size FRFs (*N*/8) clearly suffer from biased damping ratios (modal peaks affected by Hanning window), the large block size FRFs (*N*) suffer from noise. The reduced resolution FRFs (after applying a rectangular window to the IRFs) overcomes both problems.

Another approach to reduce the noise levels and leakage when estimating FRFs is proposed in [10]. Rather than applying a rectangular window to the IRFs, an exponential window is used. In this case the damping ratios need to be corrected (similar to the application of an exponential window in impact testing) instead of the participation factors.

Another idea is to use the so-called *frequency-averaging technique*: a DFT of the entire time segment is computed and afterwards the erratic spectrum is smoothed by averaging over a number of spectral lines. The benefits of this frequency-averaging technique in case of flutter testing have been demonstrated in [11].

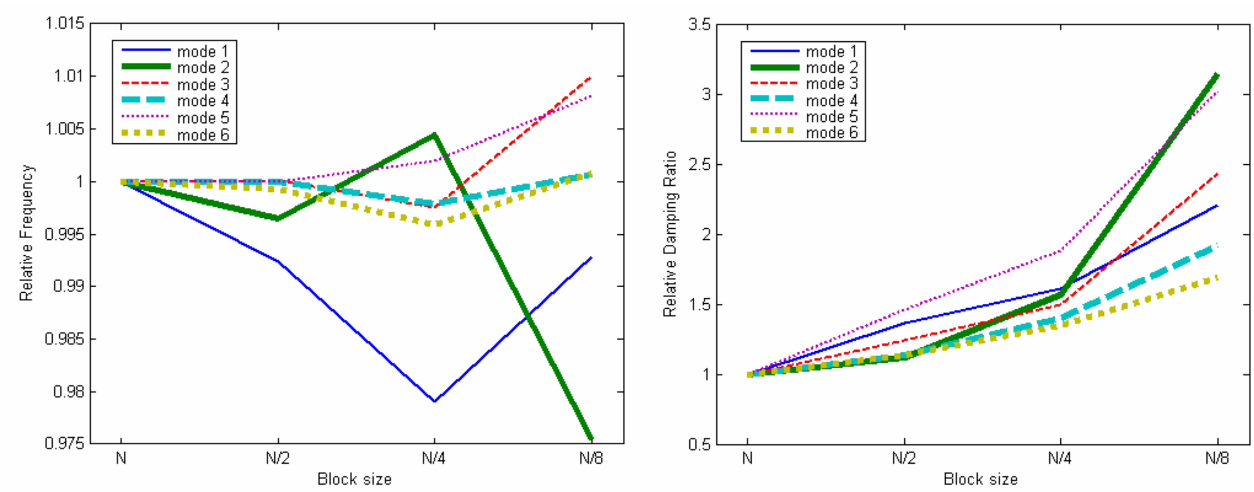

Figure 6: Relative eigenfrequencies and damping ratios for 6 modes identified from FRFs estimated with 4 different block sizes: *N*, *N*/2, *N*/4, *N*/8. All values are scaled to the values at block size *N*.

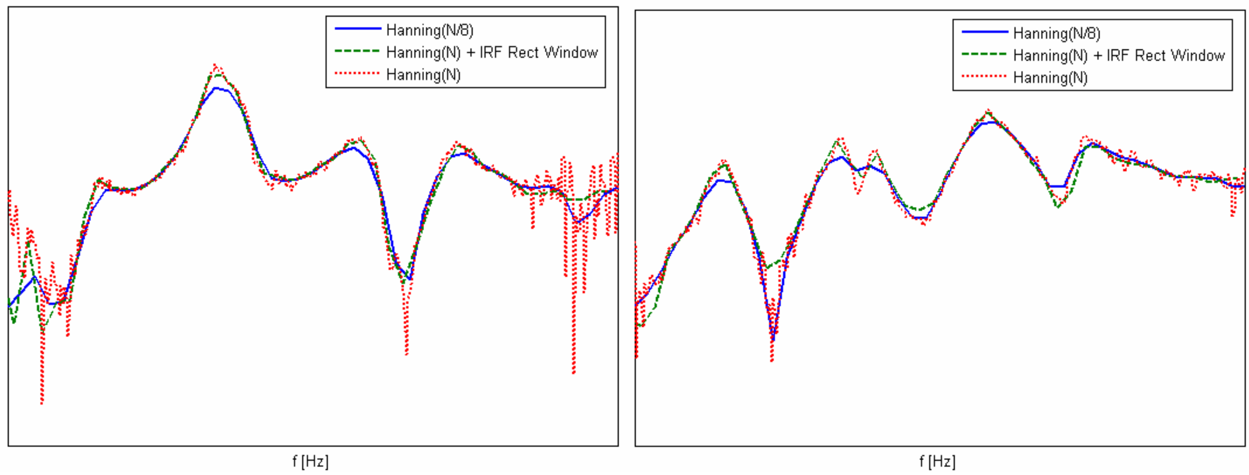

Figure 7: Comparison between FRFs obtained using different non-parametric estimation parameters. (Full – Blue) small block size *N*/8. (Dotted – Red) large block size *N*. (Dashed – Green) large block sized *N* + rectangular window applied to IRF.

4.1.3 Comparison between FRF-based frequency-domain estimators

Using the same FRF dataset (block size *N*/2, overlap 80%, Hanning window) and a fixed maximum model size (i.e. 32), the different frequency-domain estimators introduced in Section 2 are here compared with each other. The stabilization diagrams of the different methods are represented in Figure 8.

PolyMAX and PolyTLS (Poly-reference Total Least Squares) are deterministic non-iterative estimators. The other 4 are stochastic estimators, in which the variances of the FRFs (computed from the coherences) are used in the estimation as well. PolyGTLS (Poly-reference Generalized Total Least Squares) is still a non-iterative estimator. The other 3 estimators PolyBTLS, PolyIQML-LS and PolyIQML-TLS complement the initial estimates of respectively PolyGTLS, PolyMAX and PolyTLS with 1 iteration.

The difference between the LS-based and TLS-based estimators is clear. The stabilization diagrams for the PolyMAX and PolyIQML-LS are much easier to interpret than the TLS-based diagrams. The generalized eigenvalue decomposition of the PolyGTLS and PolyBTLS estimators does not seem to improve nor deteriorate the clarity of the stabilization diagram compared to the TLS estimator. The PolyTLS, PolyGTLS and PolyIQML-TLS have a lot of non-stabilizing poles.

The performance of the PolyIQML-LS estimator is promising for modal analysis applications as it combines nearly consistent estimates (the solution converges to the ML estimate) with the nice stabilization properties of a Least-Squares estimator.

Figure 9 represents the estimated values of the 6 reference modes identified at model order 32 of all 6 frequency-domain estimators of which the stabilization diagram is shown in Figure 8. Also the estimation results provided by the aircraft manufacturer are shown as the reference values (labelled as “Ref”). These reference values were obtained by applying the in-house (Laplace-domain) frequency-domain method to similar (in terms of blocksize, window, overlap length) FRFs. The differences in frequency values between the different methods are within ±3%, whereas the damping ratios vary within as much as ±45 %.

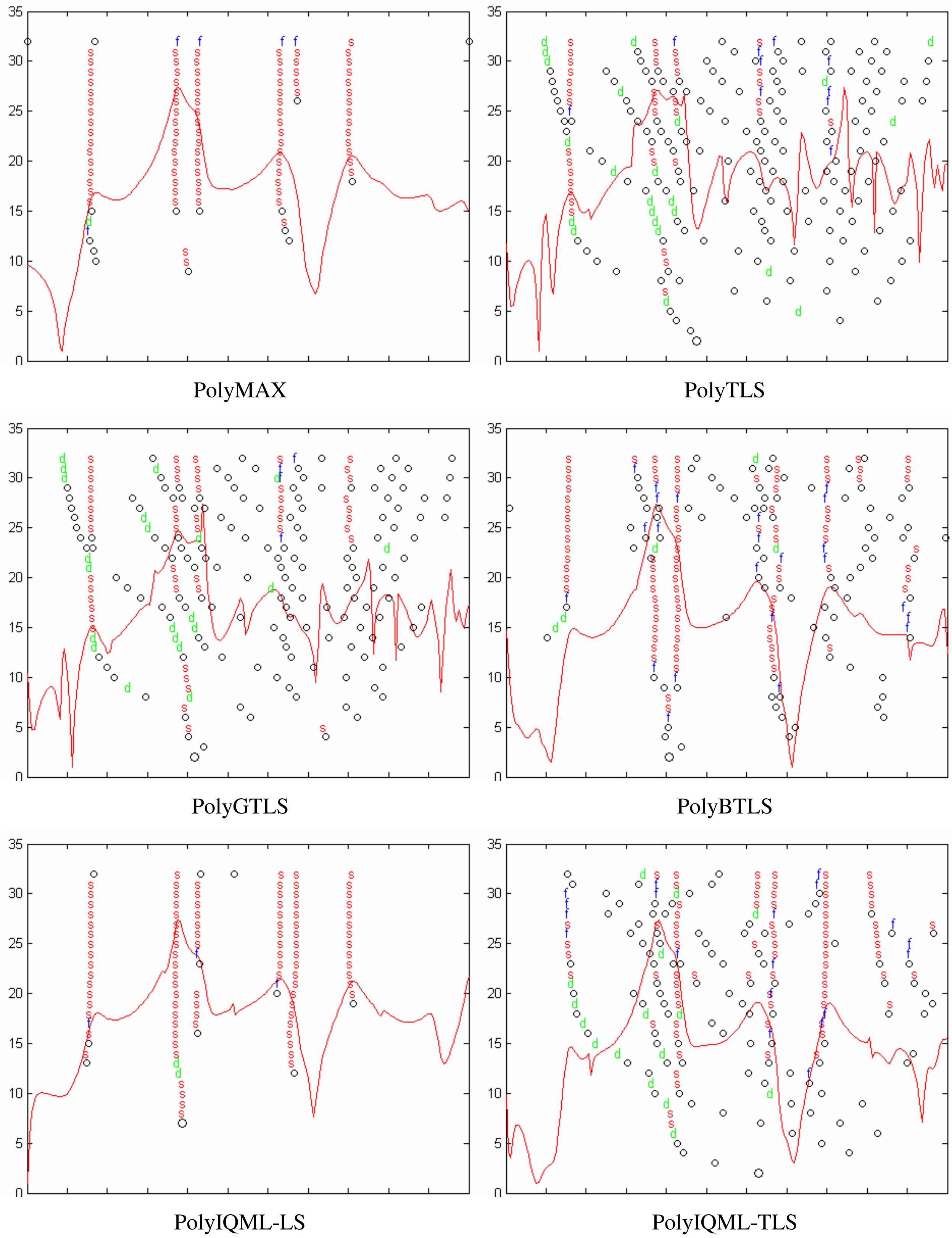

Figure 8: Stabilization diagrams of different frequency-domain estimators. The background FRF is a typical synthesized FRF based on the maximum model order 32.

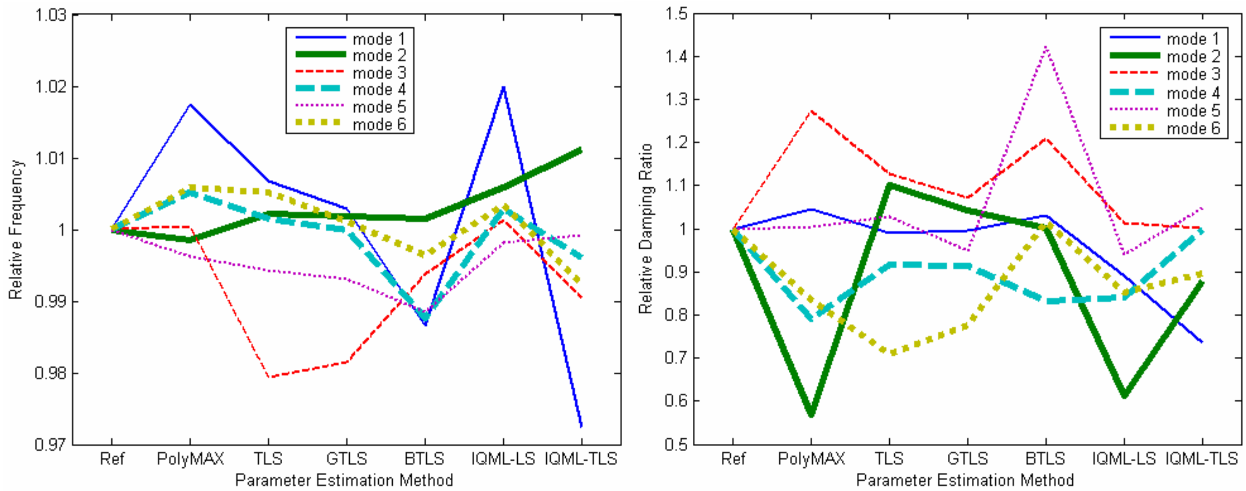

Figure 9: Relative eigenfrequencies and damping ratios for 6 modes identified using 1+6 different methods. All values are scaled by the values provided by the aircraft manufacturer (labelled as “Ref” in the graphs)

4.2 Operational modal analysis applied to turbulence response spectra

In this section, the modal parameters will be extracted from spectra which are estimated based on the turbulence-only part of the signals (Figure 1). A *leakage-free* and *Hanning-window free* pre-processing method is used to estimate the power and cross spectra. The weighted correlogram approach was adopted: correlations with positive time lags are computed from the time data; an exponential window is applied to reduce leakage and the influence of the noisier higher time lag correlation samples; and finally the DFT of the windowed correlation samples is taken. An exponential window is compatible with the modal model and therefore, the pole estimates can be corrected for the application of such a window. More details about this pre-processing and the comparison with the more classical Welch's averaged periodogram estimate (involving Hanning windows) can be found in [9][12][13].

The spectra were estimated with the same frequency resolution as the FRFs in Section 4.1. The exponential window factor applied to the auto- and cross-correlation equals 1% and 3 channels were selected as references for the computation of the cross spectra: an acceleration at the left wing tip, the right wing tip and the tail plane.

4.2.1 PolyMAX

Again, as starting point for assessing the stochastic frequency-domain estimators, the PolyMAX method is applied to 19x3 turbulence response cross spectra. Also in this case the PolyMAX stabilization diagram is very clear (Figure 10). Figure 11 confronts the measured spectra with the spectra synthesized from the estimated modal parameters. The good correspondence indicates that the major dynamic characteristics have been extracted from the data.

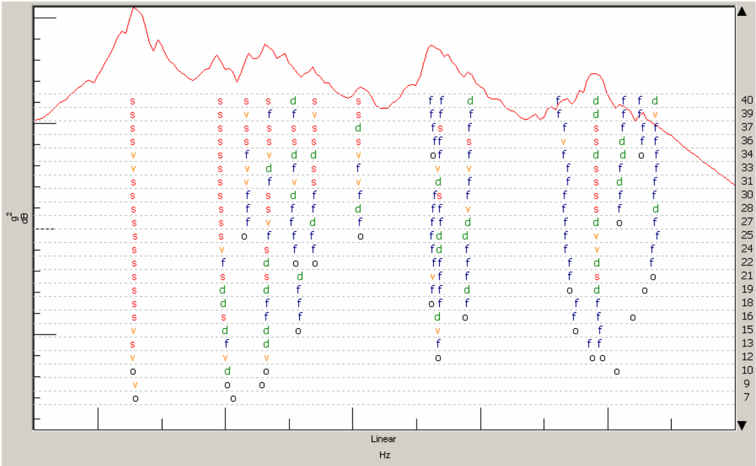

Figure 10: Stabilization diagram obtained by applying PolyMAX to in-flight aircraft data pre-processed to power and cross spectra.

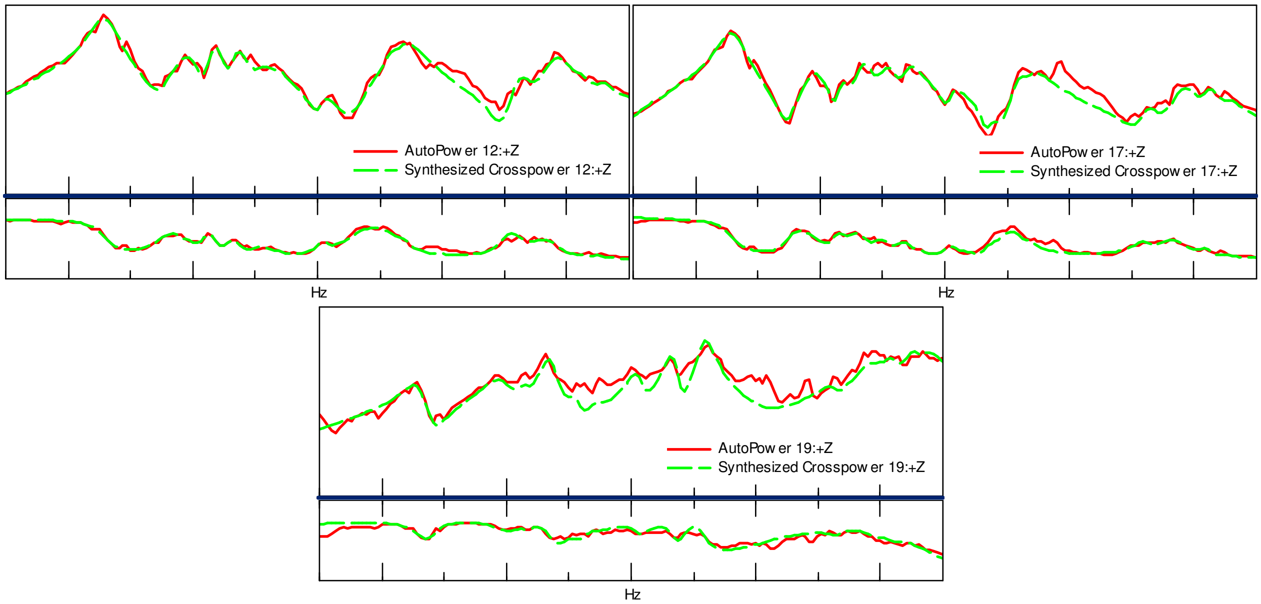

Figure 11: Measured (full – red) versus synthesized spectra (dashed – green): right wing tip – left wing tip – tail plane.

4.2.2 Comparison between spectrum-based frequency-domain estimators

In this section, the earlier introduced frequency-domain estimators are applied to the turbulence-only spectra. The stabilization diagrams of the different methods are represented in Figure 12. The maximum order of the denominator polynomial of the right matrix-fraction model is 12. As there are 3 references, the maximum number of poles is 36 (or 18 complex conjugated pairs), which is close to the model order assumed in the single-reference FRF case of Section 4.1, which was 32.

Although less horizontal lines are available in the stabilization diagrams, similar conclusions can be drawn as in the FRF case: PolyMAX and PolyIQML-LS yield the clearest diagrams. PolyIQML-LS is a stochastic estimator that requires an additional iteration step and makes use of the noise information (variance of the spectrum estimates).

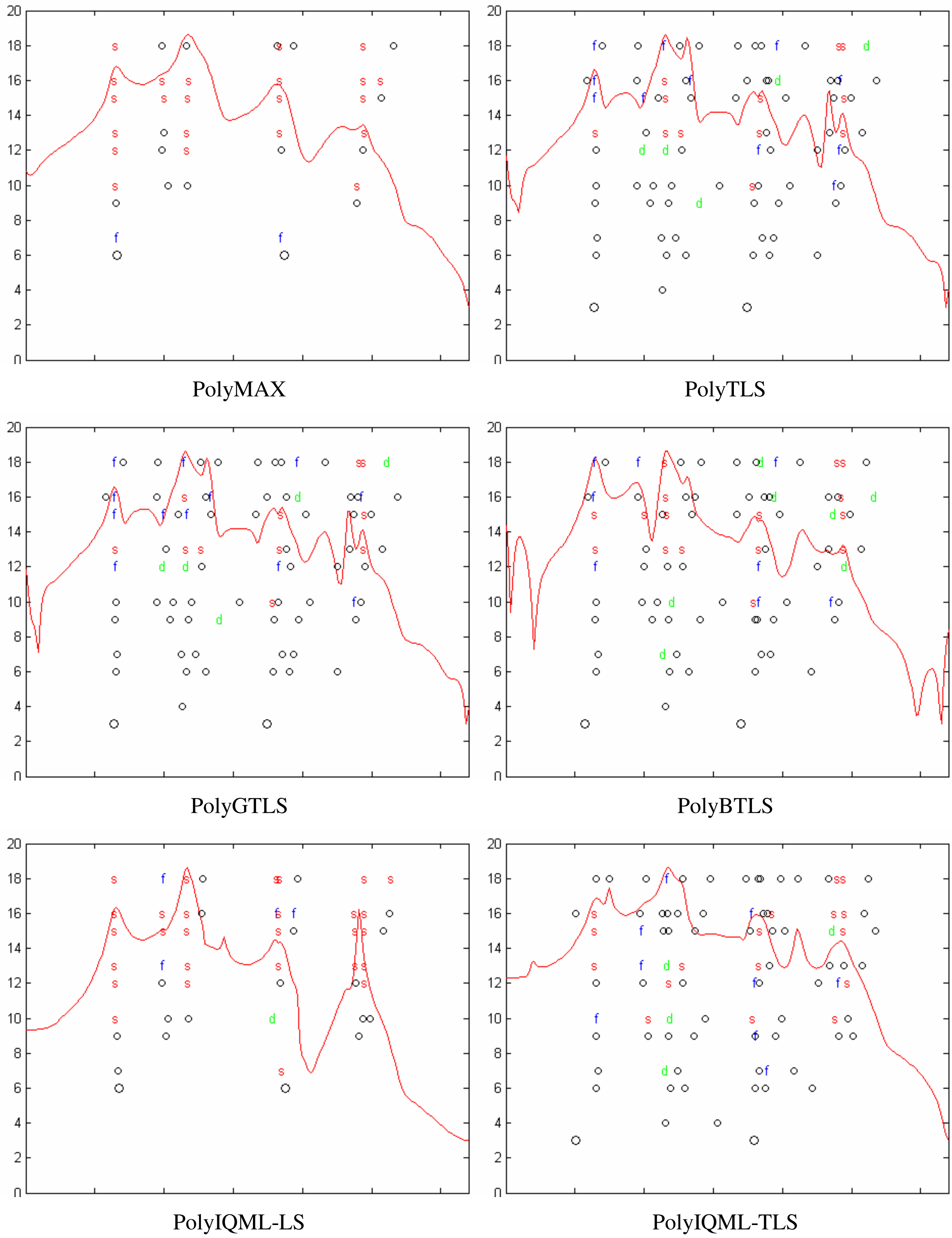

Figure 12: Stabilization diagrams of different frequency-domain estimators. The background spectrum is a typical synthesized spectrum based on the maximum model order 18.

4.3 Comparison between sweep and turbulence results

In this section the modal analysis results of both excitation types are compared: sweep versus turbulence. The comparison is restricted to the PolyMAX results, but similar conclusions can be drawn using other estimators. Table 1 compares the eigenfrequencies and damping ratios. Again, the differences are computed with respect to the values provided by the aircraft manufacturer (evidently these values are also estimated from experimental data, so they cannot be considered as “true” values). The eigenfrequencies are in good agreement; also the operational frequencies compare well with the input-output frequencies. The damping ratio differences are larger. Also, in general, the turbulence excitation damping ratios are lower than the sweep data damping ratios.

Figure 13 compares the FRF-based mode shapes with the output-only mode shapes. Except for the 5th mode, the mode shapes identified at 19 sensor locations agree very well.

Mode	Sweep data – FRF PolyMAX		Turbulence data – OMA PolyMAX	
	Relative frequency difference [%]	Relative damping ratio difference [%]	Relative frequency difference [%]	Relative damping ratio difference [%]
1	2	5	-2	-35
2	0	-43	-1	-34
3	0	27	2	5
4	1	-21	1	-43
5	0	0	1	-21
6	1	-17	2	-64

Table 1: Comparison of modal parameters identified from FRFs (sweep excitation) and spectra (turbulence excitation). Relative differences with respect to results provided by the aircraft manufacturer are considered.

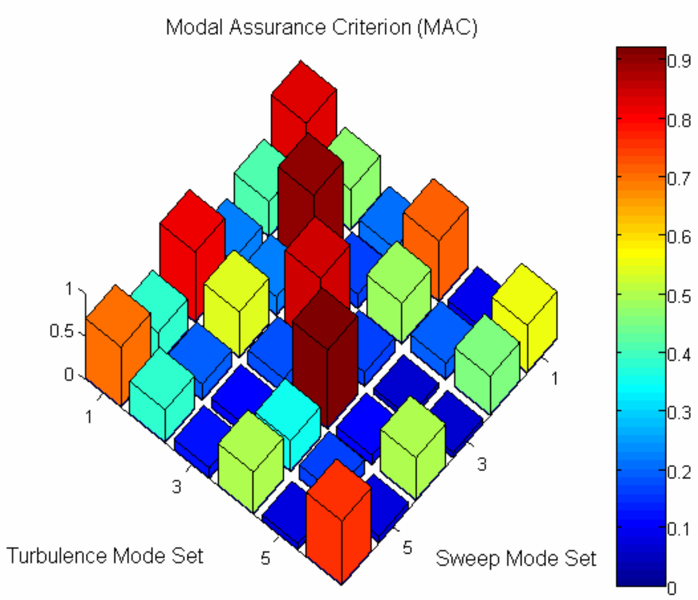

Figure 13: MAC between sweep and turbulence modes.

5 Conclusions

In this paper, some modern frequency-domain modal parameter estimation methods were applied to in-flight data of a large aircraft. The data was very interesting in the sense that in a short time interval both traditional sine sweep excitation applied at the control surfaces and natural turbulence excitation were available. It was observed that the same modes could be extracted when applying Operational Modal Analysis to the turbulence spectra as in the case of classical modal analysis applied to the sweep FRFs. When comparing different frequency-domain estimators, it is observed that the new poly-reference stochastic frequency-domain TLS estimators have the advantage that noise information is taken into account but they provide stabilization diagrams that are more difficult to interpret. The Frobenius norm constraint prohibits the use of the sign of the damping to construct clear stabilization charts. The poly-reference IQML Least-Squares estimator with particular parameter constraint combines a nice stabilization diagram and noise-corrected solutions. This estimator can be an interesting alternative for the PolyMAX estimator if noise information is available.

In this paper also a non-parametric FRF estimation method was applied that overcomes the typical trade-off between leakage and noise when processing random or single sweep data.

A final conclusion is that, despite the fact that the damping ratios are very critical parameters for flutter analysis, it was observed that rather large uncertainties are associated with this modal parameter. Depending on the data pre-processing, parameter estimation method and the used data (sweep versus turbulence) relatively large differences in damping ratios were found.

Acknowledgements

This work was carried out in the frame of the EUREKA project E! 3341 FLITE2. The financial support of the Institute for the Promotion of Innovation by Science and Technology in Flanders (IWT) is gratefully acknowledged.

References

[1] M.W. KEHOE, *A historical overview of flight flutter testing, NASA TM-4720*, **www.dfrc.nasa.gov/DTRS** (1995).

[2] C.R. PICKREL AND P.J. WHITE, Flight flutter testing of transport aircraft: in-flight modal analysis, In *Proceedings of IMAC 21, the International Modal Analysis Conference*, Kissimmee (FL), USA, February (2003).

[3] PINTELON R. AND J. SCHOUKENS, *System Identification: a Frequency Domain Approach*, New York: IEEE Press (2001).

[4] P. GUILLAUME, P. VERBOVEN, S. VANLANDUIT, H. VAN DER AUWERAER, AND B. PEETERS, A poly-reference implementation of the least-squares complex frequency-domain estimator, In *Proceedings of IMAC 21, the International Modal Analysis Conference*, Kissimmee (FL), USA, February (2003).

[5] B. PEETERS, H. VAN DER AUWERAER, P. GUILLAUME AND J. LEURIDAN, The PolyMAX Frequency-Domain Method: a New Standard for Modal Parameter Estimation?, *Shock and Vibration*, Vol.11 (2004), pp. 395-409.

[6] T. DE TROYER, P. GUILLAUME, AND G. DE SITTER, Improved poly-reference frequency-domain modal estimators for flutter analysis, In *Proceedings of SYSID 2006, the 14th IFAC Symposium on System Identification*, Newcastle, Australia (2006).

[7] T. DE TROYER AND P. GUILLAUME, Improved stabilization charts for flutter analysis using stochastic frequency-domain estimators, In *Proceedings of the 7th National Congress on Theoretical and Applied Mechanics*, Mons, Belgium (2006).

[8] R. PINTELON, P. GUILLAUME, Y. ROLAIN, J. SCHOUKENS, AND H. VAN HAMME, Parametric identification of transfer functions in the frequency domain – a survey, *IEEE Trans. Autom. Control*, Vol. 39, No. 11 (1994), pp. 2245-2260.

[9] B. CAUBERGHE, *Applied Frequency-Domain System Identification in the Field of Experimental and Operational Modal Analysis*, PhD Thesis, Vrije Universiteit Brussel (2004).

[10] P. VERBOVEN, *Frequency-Domain System Identification for Modal Analysis*, PhD thesis, Vrije Universiteit Brussel, Brussel (2002).

[11] M. MARCHITTI, Averaging spectral functions from in flight flutter signals, *Mechanical Systems and Signal Processing*, Vol. 20, No. 3 (2006), pp. 757-761.

[12] L. HERMANS, H. VAN DER AUWERAER, AND P. GUILLAUME, A frequency-domain maximum likelihood approach for the extraction of modal parameters from output-only data, In *Proceedings of ISMA23, the International Conference on Noise and Vibration Engineering*, 367-376, Leuven, Belgium, 16-18 September (1998).

[13] B. PEETERS, A. VECCHIO, AND H. VAN DER AUWERAER, PolyMAX modal parameter estimation from operational data. In *Proceedings of ISMA 2004, the International Conference on Noise and Vibration Engineering*, Leuven, Belgium, September (2004).